5.3 Positron source

5.3.1 Overview

The ILC Positron Source generates the positron beam for the ILC. To produce the positrons, the beam from the electron main linac passes through a long helical undulator to generate a multi-MeV photon beam which hits a thin metal target to generate showers of electrons and positrons. This system pushes the state-of-the-art in many areas and there has been substantial R&D on several critical items including the undulator, positron conversion target, optical matching device, photon collimator, normal conducting accelerating structures, radiation shielding and remote handling. There has also been work on the alternative conventional positron source and beamline lattice design.

5.3.2 Undulator

At the time of the *Reference Design Report* (RDR), short superconducting helical-undulator prototypes using niobium-titanium superconductors had been successfully fabricated and tested by groups at Rutherford Appleton Laboratory (RAL) in the UK and at Cornell University *[1, 2]* in the US. This gave confidence that the undulator period and field strength selected for the ILC was feasible. Since that time the RAL group has successfully fabricated two identical long undulators, each 1.75 m in length, which have been magnetically tested and proven easily to achieve the field strength required. In fact, both exceeded the magnetic field specification by more than 30% *[3]*. The quench training for the two magnets is shown in *Figure 5.3.2.1*

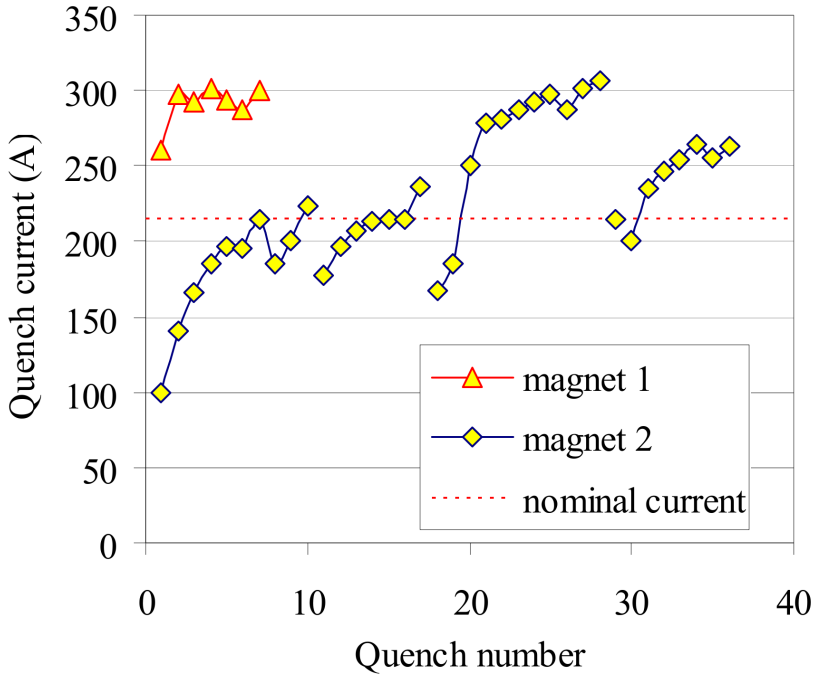

Figure 5.3.2.1 Quench history of the 2 of 1.8-m prototype superconducting helical undulator

In addition the subsequent analysis of the magnetic field results by staff at Daresbury Laboratory in the UK has shown that both undulators have a very high field quality, certainly more than sufficient to provide the intense source of photons that is required. The RAL team has since incorporated both of these undulators into a single 4-m-long cryogenic module (which operates at -269 °C) of the design required by the ILC, and has proven that both undulators can be powered simultaneously at the field levels required *[4]*. A photo of the complete undulator cryomodule is shown in *Figure 5.3.2.2.* In the future it would be valuable to test the module in an electron beam to measure the properties of the light generated by the undulators. The parameters of this undulator is given in table 5.3.2-1

Table 5.3.2-1: Parameters of ILC undulator

Undulator Type	helical
Undulator Period	11.5 mm
Undulator Strength, K	0.92,
Field on-axis	0.86 T
Beam Aperture (diameter)	5.85 mm
Winding Bore	6.35 mm

Figure 5.3.2.2 The 4-m cryostat prototype superconducting helical undulator under test at Rutherford Appleton Laboratory.

The RAL team is now investigating the use of a more advanced superconducting material, niobium tin, which should produce even higher field strengths. This would make an even shorter period undulator, which could generate the required positron yield at lower electron drive-beam energies. Currently the team is winding short prototypes to gain

experience with this technically more challenging material and also to allow a direct comparison with the other prototypes built using niobium titanium *[5]*. IAN update… Microve undulator (sami agreed to contribute)?

5.3.3 Conversion Target

The conversion target is a 1-m-diameter wheel of titanium alloy that rotates at 100 m/s at the rim. To increase the positron yield, the target rim passes through a strong magnetic field. Unfortunately, this then induces unwanted eddy currents in the wheel, causing the wheel to heat up. The level of heating that can be tolerated limits the usable magnetic field. Several groups have tried to model the eddy current heating but consistent now. t results were obtained from the different simulation codes used *[6,7]*. Consequently a full-scale prototype target was built at the Cockcroft Institute in the UK to benchmark the simulation codes. The target wheel was fabricated from the required titanium alloy and was rotated over a range of rim velocities in a strong magnetic field (Figure 5.3.3-1). The results of this unique experiment have accurately quantified the eddy current effects and have confirmed which simulations were correct [8]. Furthermore, the experiment has proven that the magnetic field level assumed by the positron source design at the target wheel is feasible, with the eddy current heating being easily tolerated.

The target wheel also has to operate inside a vacuum chamber while the motor is in air. This means that a rotating vacuum seal is required that is capable of operating at high velocity, near a magnet and in a high radiation environment – quite a demanding challenge. The team has identified a commercial vacuum seal that appears suitable for ILC conditions. To confirm the long-term performance of the seal, a relatively simple test is currently being underway by staff at Lawrence Livermore National Laboratory (LLNL) in the US. Initially, an equivalent load to the target will be rotated in a vacuum and the performance of the seal evaluated by monitoring the vacuum level within the chamber. Later the full-size target wheel devliverd from the Cockcroft Institute to LLNL, and be rotated at the speeds required by the ILC under vacuum. The engineering design concept for this test is shown in *Figure 5.3.3-2.*

Figure 5.3.3-1 Prototype rotating target setup for eddy current tests at Daresbury Lab. Copyright STFC.

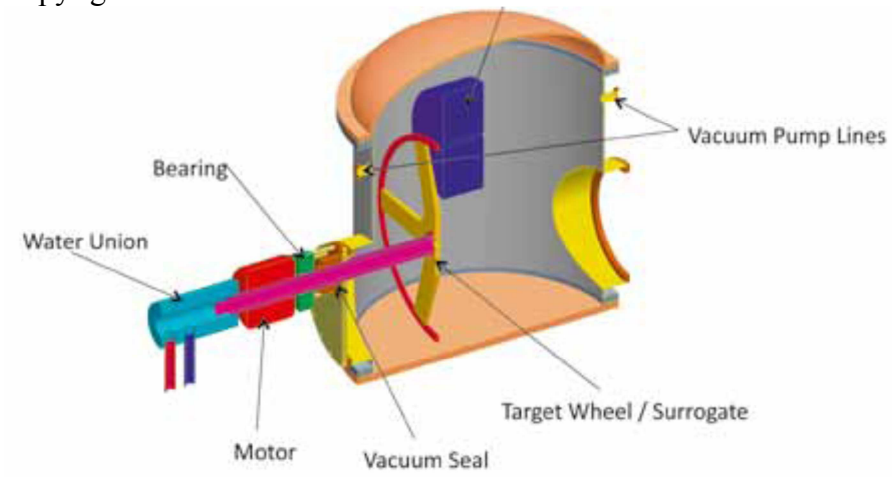

Figure 5.3.3-2 Schematic of the engineering design for the in-vacuum rotating target.

Another issue for the target that is the effect of the shockwave on the target as a consequence of being struck by the intense pulses of gamma photons generated by the undulator *[8]*. Concerns were raised over possible material damage to the target itself on a shot-by-shot basis. Simulations with a numerical code at LLNL suggested that the effect is not significant. This has since been confirmed with a detailed analytical study, carried out at Durham University in the UK *[9]*.

Conclusion: vacuum test ongoing, looks promising, remaining RD will answer, maybe differential pumping is needed in addition.
Gudi: futher study ongoing on material damages at DESY and Hamburg Univ.

5.3.4 OMD

The flux concentrator is the pulsed magnet that generates the strong magnetic field close to the target wheel in order to enhance the positron yield. Many of these have been used successfully in the past but the parameters of the ILC are more technically challenging. A detailed R&D study has been initiated at LLNL to confirm the feasibility of the proposed magnet and later to build a suitable prototype to demonstrate the design performance. The design is now well advanced (shown in *Figure 5.3.4-1* with the field profile in *Figure 5.3.4-2)* and the simulations predict excellent performance of the magnet *[10]*. which operates at room temperature using a water cooled coil and disk(see Figure 5.3.4-3). In this design, the device sits in vacuum; all power and cooling connections move to the rim; the coils are kapton wound, hollow copper and water cooled; the plates are OFHC copper with water cooling pipes soldered in; there is only metal in the high radiation areas; plates and coils are stacked and bolted together. With the help of a pulse forming network, the flux concentrator B field has a much better flat top than the previous design(see Figure 5.3.4-3b).

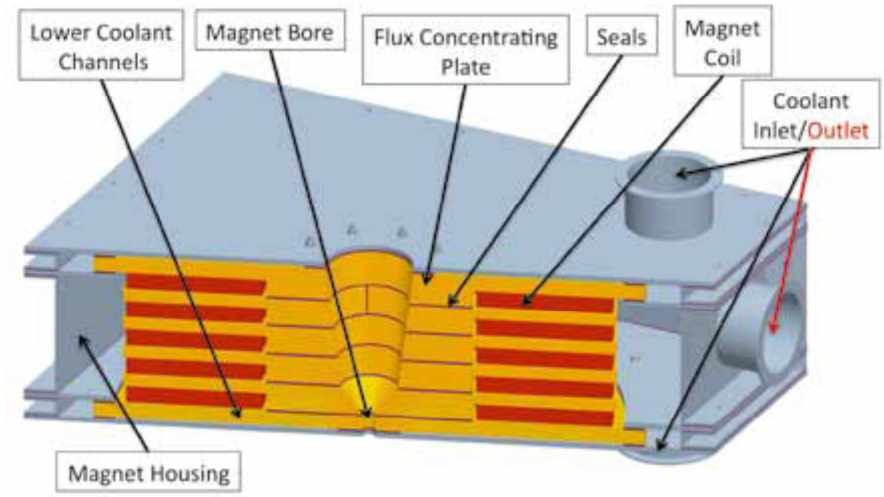

Figure 5.3.4-1 Section of the prototype design for the pulsed flux concentrator.

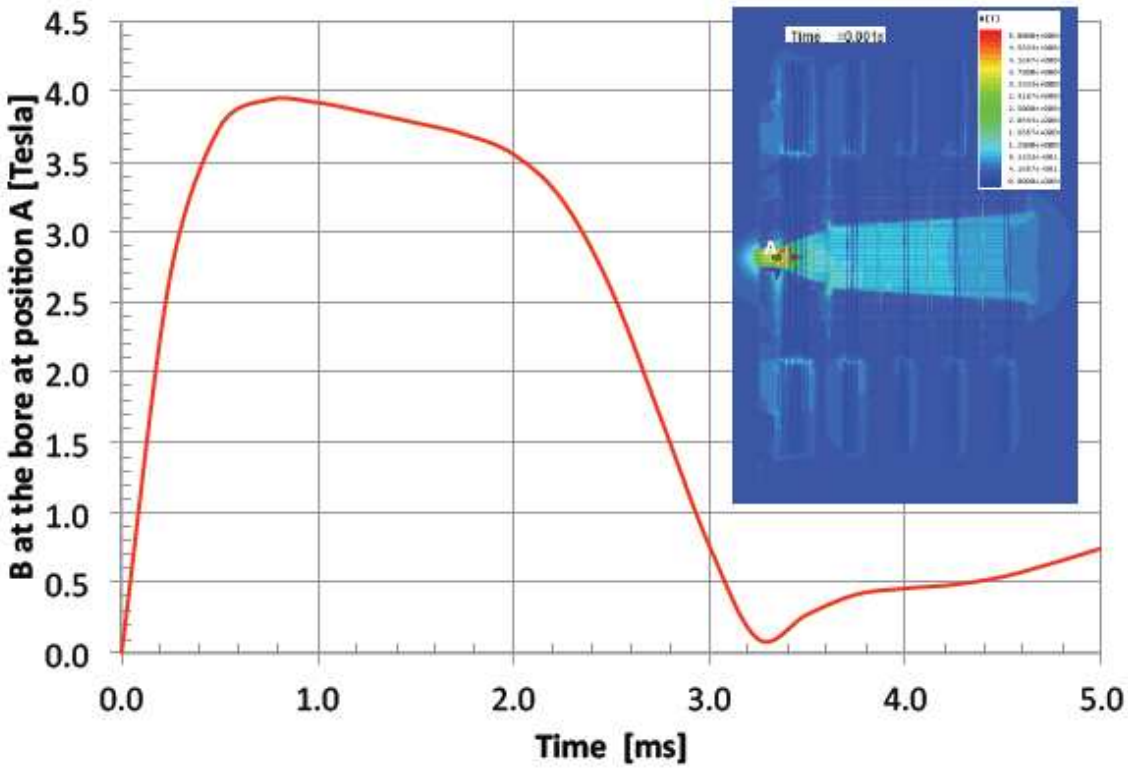

Figure 5.3.4-2 B field profile of the pulsed flux concentrator with wave form correction implemnedrted

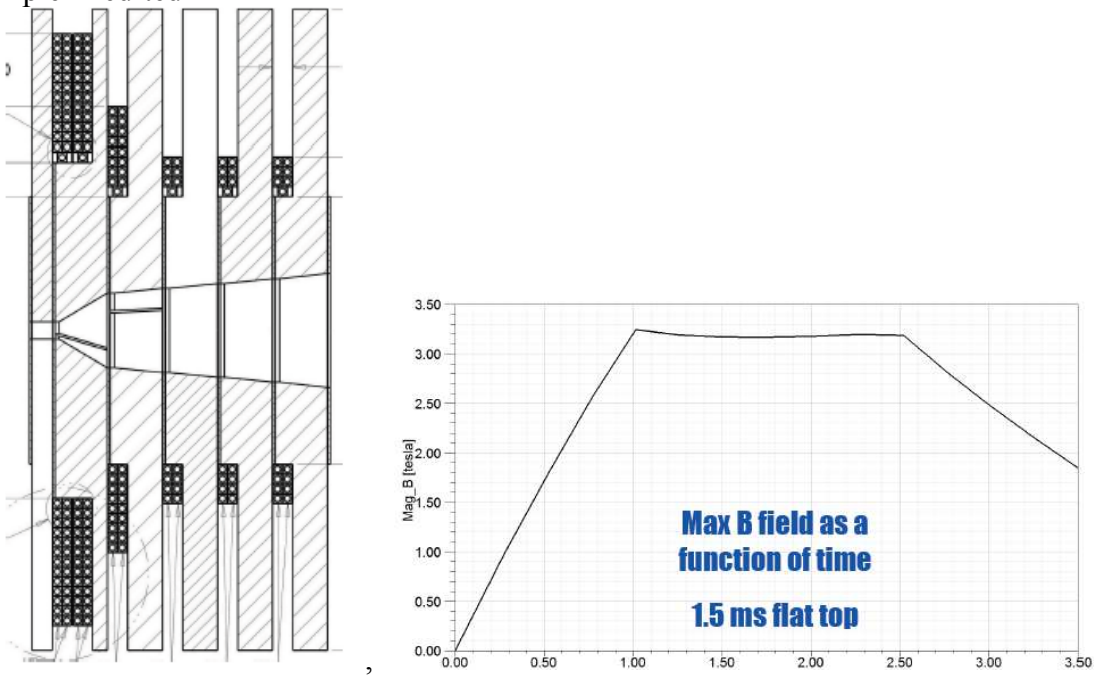

Figure 5.3.4.3: Drawing of new room temperature flux concentrator and its designed B field pulse

5.3.5 Photon collimator

The positron beam polarization of ~30% can be increased to 50-60% with a photon collimator upstream of the target. This reduces the number of photons which has to be compensated by a longer active undulator length up to 231? meters. (physical length too?). The collimator must withstand a large heat load as well as a huge peak energy deposition density. Table 1 summarizes the basic requirements for the photon collimator depending on the center-of-mass energy and the undulator parameters based on a positron yield of Y=1.5 e^+/e^-.

Table 1: Basic requirements for the photon collimator at the positron source and resulting degree of positron polarization. The number of bunches is 1312 with a bunch population of 2×10^{10} positrons; the positron yield is Y=1.5 e^+/e^- for the smallest aperture of the final collimator

Parameter	Unit	Center-of-mass energy, E_{cm} [GeV]			
		200−250	350	500	500
Drive electron beam energy	GeV	150	175	250	250
Undulator K value		0.92			
Undulator period λ_u	cm	1.15			
Positron polarization	%	55	59	50	59
Collimator iris radius	mm	2	1.4	1	0.7
Active undulator length	m	231	196	70	144
Photon beam power	kW	98.4	113.4	82.4	173
Power absorbed in collimator	kW	39.4	60.1	35.8	100
Power absorbed in collimator	%	40	50.3	43.5	57.8

The collimator parameters, in particular the collimator iris radius, are coupled to the drive beam energy. Hence, instead of a universal collimator for the whole center-of-mass energy range a multi-stage collimator design with decreasing iris is used. Each stage is constructed from the same materials but has different lengths to absorb the part of the photon beam with lower polarization. The first and longest section of the collimator is made of pyrolytic Carbon. This is followed by layers of materials with increasing Z, Titanium, Iron and Tungsten, which stop the shower and reduce the intensity of the absorbed photon beam to less than 0.1% after the final collimator. Each section must be long enough to reduce the power to a value which can be handled by the next section. Conical bores in the Carbon and Titanium parts ensure a smooth heat load distribution over a large region. The average heat load as well as the peak values of the energy deposition (PEDD) in the material are below the recommended stress limits.

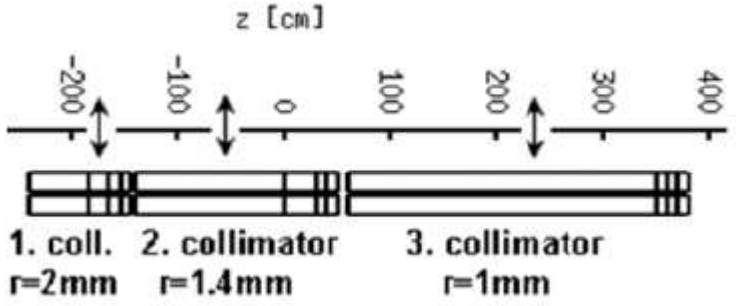

Figure 5.3.5-1: Basic layout of the multi-stage photon collimator at the positron source

A sketch of the collimator layout is presented in figure 5.3.5-5.3.5-1. Each collimator stage can be moved onto or off of the beamline. The maximum energy deposition in the collimator materials is summarized in table 2. For the luminosity upgrade at *Ecm*=500 GeV, the values given in the last column of table 2 have to be doubled.

Table 2: The peak power densities deposited in the components of the first (r=2mm), second (r=1.4mm) and third (r=1mm) collimator stage for different center-of-mass energies and degrees of polarization. The number of bunches is 1312 with a bunch population of 2×10^{10} positrons; the positron yield is Y=1.5 e^+/e^- for the smallest aperture of the final collimator. (make it clear that 10 Hy is usd for low energy)

Parameter	Unit	Center-of-mass energy E_{cm} [GeV]					
		200 – 250	350		500		
iris radius r	mm	2	2	1.4	2	1.4	1
e^+ polarization	%	55	59		50		
max. energy density in							
pyrolytic C	J/g	154	139	129	38.3	54.3	60.4
Titan	J/g	41.3	37.1	15.8	9.6	9.6	10
Iron	J/g	23.3	24.2	12.5	8.0	7.2	8.4
Tungsten	J/g	3.6	3.9	1.7	1.4	1.1	1.6
average cooling power	kW/m^2	41	35*	25*	13.6	13.2	10.3

The dimensions of the collimator stages, the average heat load in the sections and the corresponding cooling power are given in table 3. The outer diameter is 20–30cm. Due to radiation activation, remote handling will be required. Jusat as target system.

Table 3: Lengths of the photon collimator parts for the three stages

Parameter	Unit	1. collimator (r=2mm)	2. collimator (r=1.4mm)	3. collimator (r=1mm)
length of				
pyrolytic C	cm	55	140	290
Titan	cm	20	30	10
Iron	cm	10	10	10
Tungsten	cm	10	10	10

Conclusion: Are we OK? Further RD and engineering design on realistic collimators are needed.

5.3.6 Normal conducting RF accelerating structure prototyping and RF breakdown Study

Due to the extremely high energy deposition from positrons, electrons, photons and neutrons behind the positron target, the 1.3 GHz pre-accelerator has to use normal conducting structures up to an energy of 400 MeV. Major challenges are achieving adequate cooling with the high RF and particle loss heating, and sustaining high accelerator gradients during millisecond-long pulses in a strong magnetic field. The positron capture section contains both standing-wave (SW) and traveling-wave (TW) L-band accelerator structures. Detail about the parameters of these standing wave and travelling wave L-band accelerator structures can be found in TDR2.

A half-length (5-cell) prototype standing-wave (SW), cavity was built at SLAC to verify that the gradient (15 MV/m in 1.0 ms pulses) can be achieved stably and without significant detuning from the RF heat load (4 kW per cell). The cavity cross-section is shown in Fig. 5.3.6-4. Fig. 5.3.6-5 is a plot of the cold test measurement of the mode frequencies (dots); the solid line is the fitted dispersion curve. The unloaded Q of the cavity is ~ 29000 and the operating frequency (at π phase advance) is 1299.7 MHz. The time constant of this critically-coupled cavity ($0.5Q_o/\omega$) is 1.8 us.

The cavity has been rf processed at the π-mode for about 530 hrs and it has incurred about 6200 breakdowns. The gradient goal of 15 MV/m with 1 ms pulses has been achieved. Fig. 5.3.6-6 shows the breakdown rate history during processing. For these data, the pulse repetition rate was 5 Hz except for 1 ms pulses where it was lowered to 1 Hz to reduce the detuning as the reflected power was causing waveguide breakdowns (the source of these breakdowns has since been eliminated and 5 Hz operation is expected to be possible in the future). The cooling system was designed to have about 25% reflected power when the cavity was turned on 'cold' that then dropped to zero in steady state with full rf power dissipation (20 kW at 15 MV/m). In this way, a cavity temperature control system is not needed (at least for testing). However, the flow rate that was achieved (due to a limited supply of temperature regulated water) was 86 gpm compared to the 140 gpm desired, which increased the cavity temperature by about 50% (to 0.13 degC per kW dissipated). Also, the detuning (-2.7 kHz/kW) was about 25% larger than expected from simulations using the actual temperature rise and led to an overall reflection of about 50% when cold with the appropriate choice of rf frequency to minimize the reflection at full power in steady state.

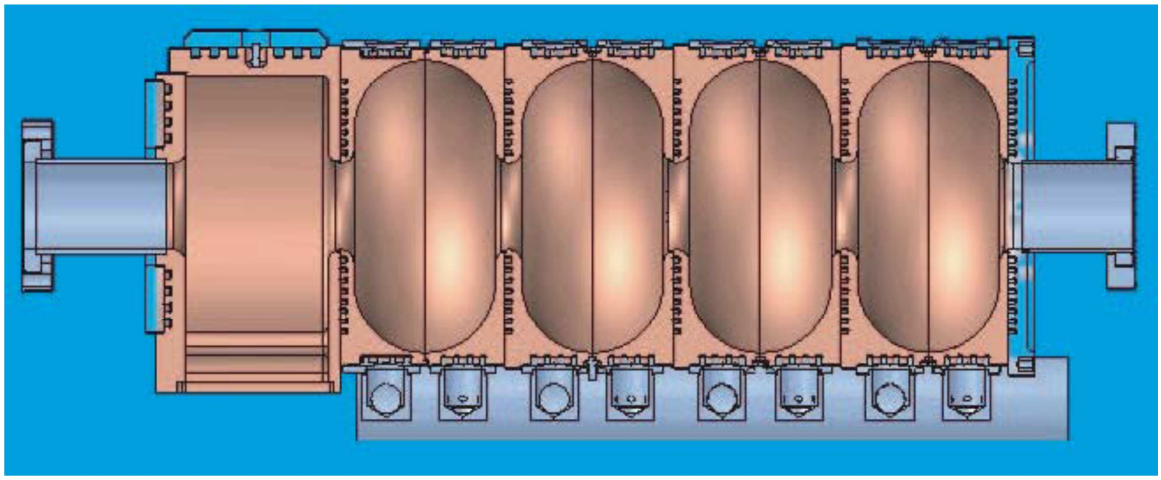

Figure 5.3.6-4 Cross section of 5cell standing wave cavity with cooling channels

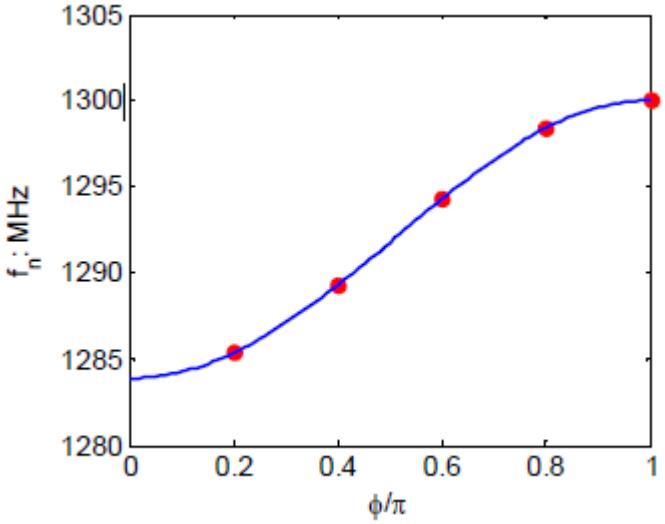

Figure 5.3.6-5 The 5 cell standing wave linac dispersion curve

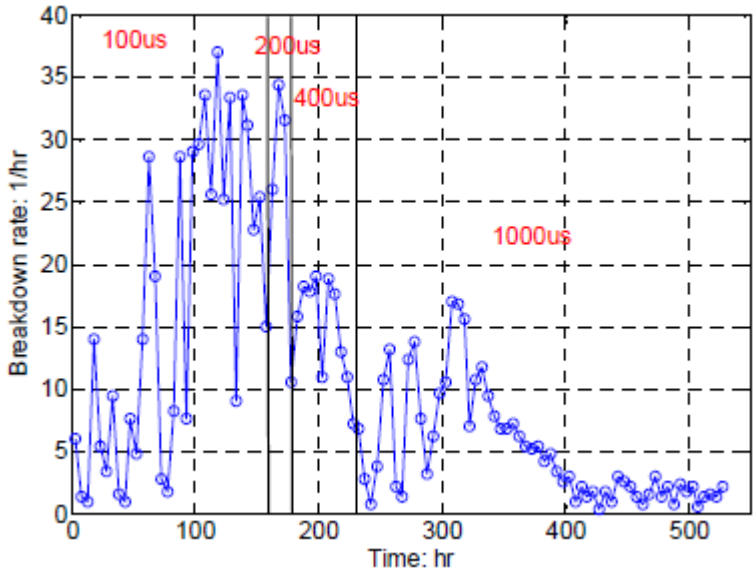

Figure 5.3.6-6 breakdown rate history of the cavity with different pulse length

After hundreds of hours of conditioning, the breakdown rate was measured as a function of unloaded gradient (G), as shown in Fig. 5.3.6-6. A G^{21} dependence was found, which is less steep than the G^{32} dependence recently observed for a CERN-designed, low a/λ, TW, X-band (11.4 GHz) structure . However, the gradient exponent is within the 20-30 range measured for NLC/GLC X-band prototype structures and close to the 19.5 value measured for the FNAL 805 MHz injector linac cavities.

5.3.7 Performance simulation

The parameters for source subsystems and the determination of the source performance can only be quantified using complex simulations. These simulations quite often require the combination of several sophisticated computer codes. The primary performance figure of merit is the yield, defined as the number of positrons captured in the acceptance of the damping ring per electron passing through the undulator. (Ideally a yield of 1 is required, but the design goal is set at 1.5 to allow a 50% safety factor.) The second figure of merit is the polarization of the captured positrons, which depends on additional parameters such as the collimation aperture of the photon beam before the target.

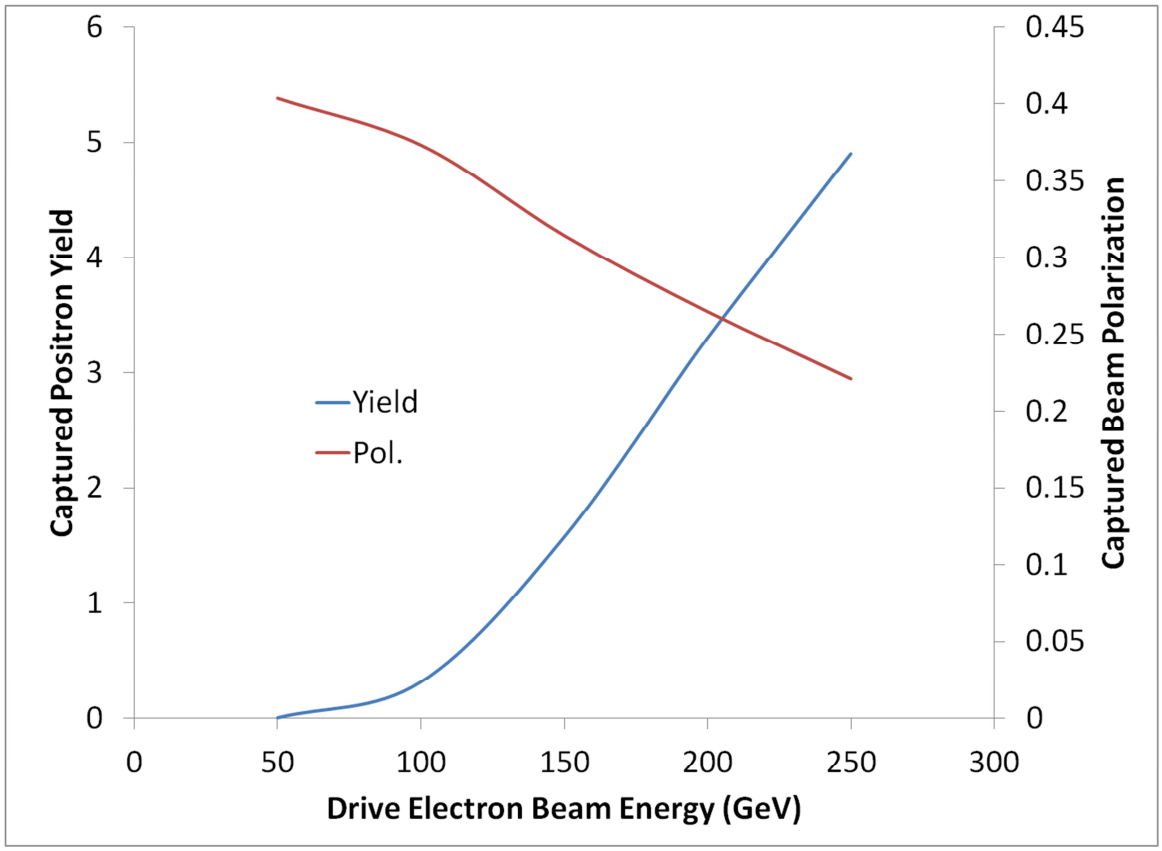

{caption:Simulation results of positron source yield and polarization for RDR undulator with QWT as OMD.} {label:figps81} check for consistences.

As shown in Figure{ref:figps81} and TDR2 Figure 3.3, for a given undulator and positron capturing system the performance of the positron source strongly depends on the energy of the main electron beam. At higher energy, the undulator B field is reoptimized to restore the polarization to 30% The final parameters are listed in TDR2 table 3.2. Performance simulation studies have also been done to determine the target energy deposition and the impact of the undulator on the electron beam parameters.[12,13]

5.3.8 Lattice design

As shown in Figure 5.3.8-1, The layout of the ILC positron source beamline is shown in TDR2 Figure 3.2 and the optics functions are shown in TDR2 Figure 3.6.

The lattice downstream of the separation chicane and through the transport line is the same as in the RDR. The quad settings of the FODO transport lattice have been re-optimized to minimize emittance growth and maximize transmission. The booster Linac lattice has been redesigned around the real geometry of cryomodules. The Linac to Ring lattice has also been redesigned to adapt to the central region integration .

5.3.9 Remote handling and radiation shielding

The target will be highly activated after a year of operation.gien some design credit to RAL on their initial design. Calculations show that with the nominal 150 kW photon beam, after 5000 hours of operation and 1 week of shutdown, the equivalent dose rate at 1 m from the target wheel will be approximately 170 mSv/h. Concrete shielding 0.8m thick around the target is thought to be sufficient to fully contain the radiation associated with the beam and with the subsequently activated materials. Additional shielding may be needed upstream and downstream of the target and around the beam dump. Figure 5.3.9-1 shows the calculation results for the target activation and required shielding.

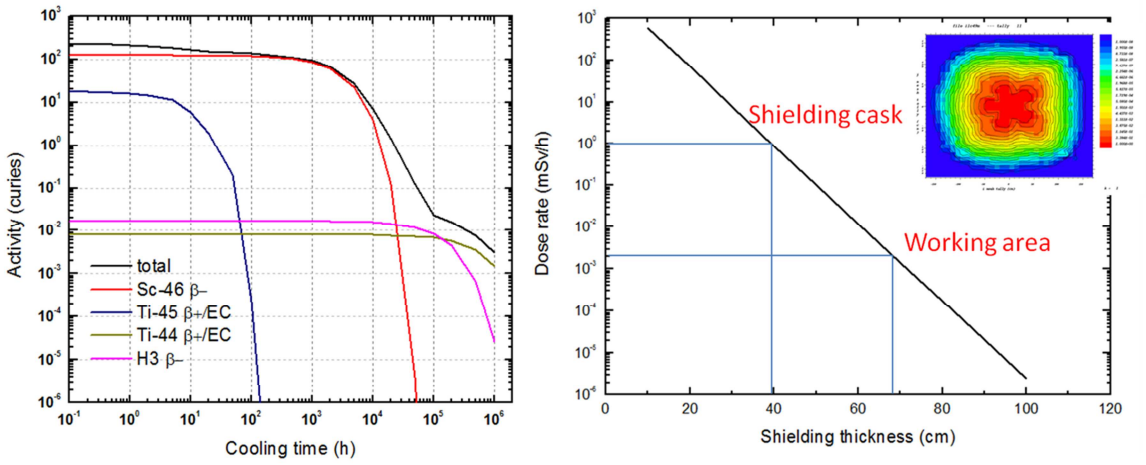

Figure 5.3.9-1 shielding calculation for used target

A remote-handling system is used to replace the target, OMD and 1.3 meter NC RF cavities. To minimize time for a target exchange, the whole target system is designed into a plug with the top shielding. The interfaces of the target plug with the two beamlines are inflatable seals for the vacuum enclosure. The actual disconnection and reconnection of the target would be done locally, and then the targets removed and replaced vertically by an overhead crane. The used target is placed into a shielding cask for storage until the radiation has decayed to a safe level. **Figure 5.3.9-2** shows the conceptual design of such a system. Estimatwed change over time, (?),

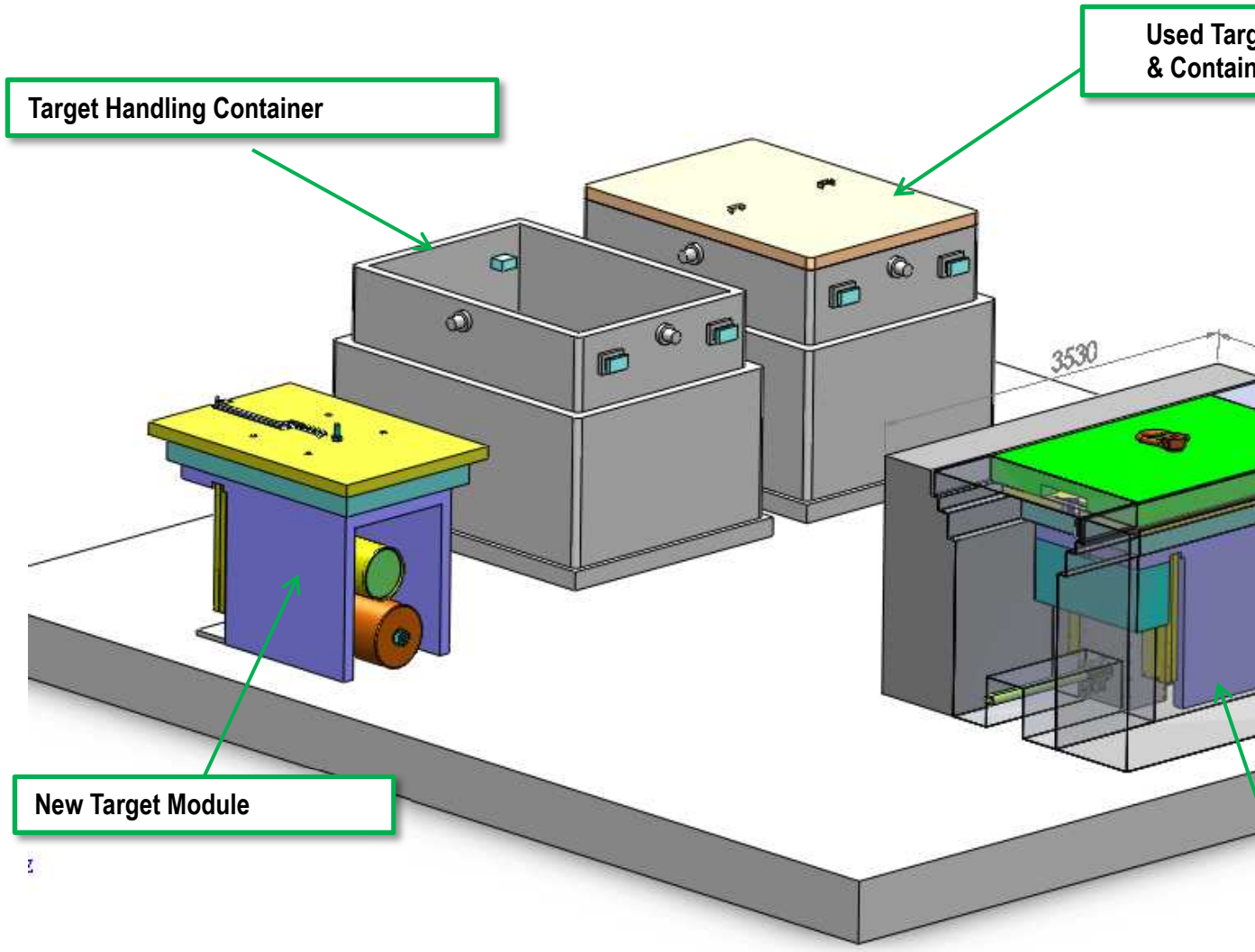

Figure 5.3.9-2 General layout for used target remote handling concept

5.3.10 Alternative source

Two alternative positron sources are being investigated. First is the conventional positron source[1]. Since the undulator-based source represents a novel concept the more

conventional option using an electron beam on a thick target is also being investigated as possible backup solution. Second is laser Compton based polarized positron source as a possible future advanced scheme[2]. Though conventional and Compton options are quite different approach, both have a common feature which is the independence from other systems. The independence of the both alternative systems is an advantage over the undulator scheme. The undulator-based source gives interconnection to nearly all sub-systems of the ILC, because it uses electron beam in the electron main linac to produce positrons. A large-scale interconnected system is a challenge and strict constraints are given to the positron source and the target heat load by the time structure of the beams. The alternative sources are free from such constraints.

300 Hz Conventional source:

We employ stretching of the pulse length of a bunch-train in positron generation to ease target thermal and shockwave issues. The schematic view of the 300 Hz scheme is shown in Fig.1. The point is that, in ILC, the bunch timing structures and pulse timing structures can be different in the positron source, in the DR, and in the main linac. So we have some flexibility to choose timing structures in positron source and we use it for time stretching. The repetition rate of ILC main linac is 5 Hz, therefore there in an interval of 200 ms between two pulses. This gives us enough time for pulse stretching. We employ a normal conducting 300 Hz electron linac to create positrons. The pulse to pulse separation of the linac is 3.3 ms. Each pulse of the 300 Hz linac creates about 130 bunches, so 20 linac pulses create 2600 bunches of positron in about 63 m seconds.

The bunch-to-bunch separation of 6.15 ns in the 300 Hz linac is chosen, because the bunch-to-bunch separation in the damping ring is 6.15 ns. To match the mini-train beam structure of the damping ring, in the 300 Hz linac, one RF pulse accelerates three mini-trains with inter-mini-train gaps. This package of three mini-trains is named triplet. Each mini-train contains 44 bunches. With 6.15 ns bunch-to-bunch separation and 44 bunches per mini-train, the length of a mini-train is 264 ns. Since a triplet contains three mini-trains, it consists of 132 bunches and we need 20 triplets to form 2640 bunches. There are gaps of about 100 ns between the mini-trains in a triplet. The gap is necessary to prevent the instability caused by electron clouds in the damping ring.

As a whole the beam parameter assumed in the conventional source is the ILC nominal beam parameter, but with slight modifications. In the original ILC nominal parameter set, one RF pulse in the main linac has 2625 bunches. Here, we assume 2640 bunches per pulse.

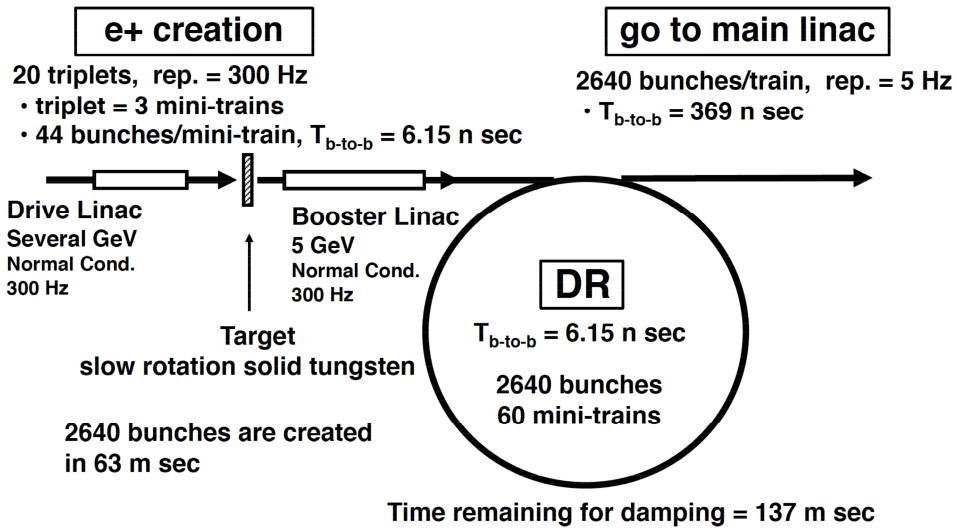

Figure 1. Schematic view of the 300 Hz positron generation scheme. The repetition rate of the drive linac and the booster linac is 300 Hz, whereas the repetition rate of the main linac is 5 Hz.

In addition to employ the 300-Hz-generation, it is important to optimize the drive beam and target parameters to reduce target thermal issues. An intense simulation study was performed and it was concluded that a single production target made of tungsten alloy can be employed in the conventional source if we employ appropriate parameter. Typical choice of the drive beam parameters are a bunch charge of 3.2 nC, energy of 6 GeV, and R.M.S. spot size on the target of 4 mm. With the chosen drive beam parameters the optimal target thickness is 14 mm. The slow rotation is enough to deal with the thermal load. Typically we assume the tangential speed of 0.5-1 m/s. The rotation peed is much slower than that of the undulator-based positron source.

At the downstream of the target, there is a positron capture system consists of an Adiabatic Matching Device (AMD) and a RF-section. The RF-section is a L-band accelerating structure. We assume a flux concentrator as an AMD. In the 300 Hz scheme, the pulse length of the triplet is about 1 μs. Therefore pulse length of the flux concentrator is also about 1 μs. The 1 μs pulse length is similar to that of existing flux concentrators. So the technology already exists. Further, the pulse length is short enough to use a high acceleration gradient of the RF-section. After exiting the capture section, the positron energy is boosted to 5 GeV in a 300 Hz normal conducting linac. Then kicker with pulse length of about 1 μs and repetition rate 300 Hz is employed to send the positrons to the DR. One kicker pulse sends a triplet to DR. The kicker with 1 μs pulse length can be build with existing technology After the damping, each bunch is extracted from the DR by the fast kicker, sent to the bunch compressor, and sent to the main linac. The fast kicker has a capability of bunch-by-bunch extraction. The fast kicker remains the same as in the ILC baseline design with an undulator positron source. The bunch-to-bunch separation is 369 ns after the extraction.

Compton Sources:

There are three schemes for polarized positron beam generation based on the inverse-Compton scattering. They are called Ring-Compton, ERL-Compton, and Linac-Compton. The Ring-Compton consists of a 1.8GeV Linac, a 1.8 GeV storage ring with five Compton interaction points (IPs) at which an optical cavity is installed to keep laser pulse of 600mJ in it. Bunch charge of the ring is 5.3 nC and bunch spacing is 6.15 ns. In the ERL Compton scheme, ERL is employed as the dedicated electron driver which accelerates 480pC bunched beam up to 1.8GeV with bunch spacing of 18.5ns. Then, multi-bunch beam collides the laser pulse of 600mJ at five IPs at which an optical cavity is installed to keep 600mJ laser pulse.

The three polarized Compton source should be matched to the 300Hz normal Linac for the smooth change from non-polarized to high polarized positron source.

Linac Compton will be smoothly replaced if the reliability of the CO2 laser technology and the heavy beam loading compensation scheme of the linac will be confirmed. The 6 GeV 300 Hz drive linac of the conventional scheme is reused with the updgrad for the driver. At the end of the linac, Compton IPs are placed, followed by the positron production target. The 5 GeV booster linac is also reused.

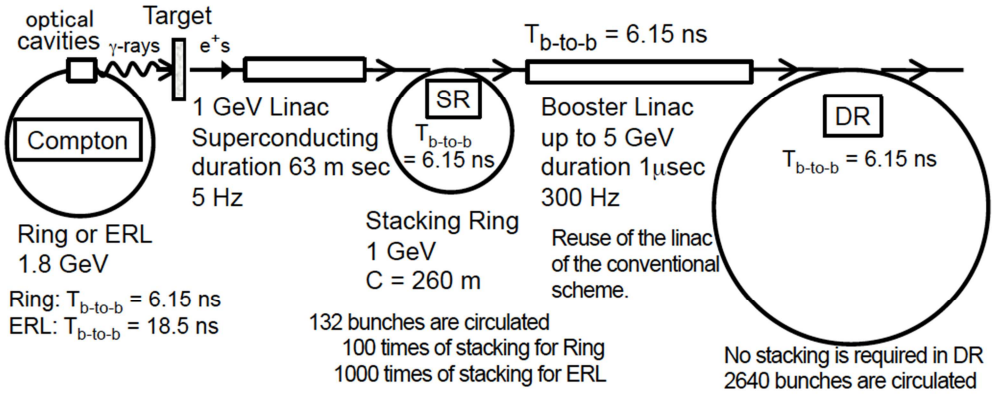

Fig 2. The conceptual design of Ring-Compton and ERL-Compton which can be applicable for the future upgrade from the 300 Hz conventional positron source.

Hereafter, Ring-Compton and ERL-Compton are discussed. Fig. 2 shows the schematic layout of the Ring- and ERL-Compton schemes. Timing structures of them are presented in Fig. 3. First, common feature of Ring- and ERL-Compton are described. The 6 GeV 300 Hz drive linac is removed, but the 5 GeV 300 Hz linac is reused. Positrons produced by the polarized gamma-rays are accelerated upto 1 GeV by the superconducting linac then injected into the 1 GeV stacking ring. The linac operates at 5 Hz and has a long duration of 63 m sec. Then the 1 GeV stacking ring with about 260m circumference is

employed. In the stacking ring, 132 bunchs are stored with 6.15 ns bunch spacing*. The 132 bunches are sent to the booster linac at once by a kicker which pulse length is 1 micro seconds. The booster linac is normal conducting. It has heavy beam loading ($3x10^{10}$ positrons/bunch) and operated with about 1 μ sec pulse duration at 300 Hz. 20 times beam extraction from the stacking ring makes 2640 bunches in the damping ring. No stacking is necessary in the damping ring.

Regarding Ring-Compton, we need 100 times positron bunch stacking in the same bunch in the staking ring. Since the bunch spacing in the Compton ring and in the staking ring is the same, 100 times of stacking need 100 turns in the sacking ring. It takes about 87 μ s, because the circumference of the ring is 260 m. We take cooling period of 3.2ms after stacking for stable operation of the Compton ring and the stacking ring. Total period of one cycle is 3.3 m sec (300 Hz). 20 times beam extraction takes 63ms.

Regarding ERL Compton, we need 1000 times of the stacking in the same bunch in the stacking ring. The bunch separation in ERL is 18.5 n sec. Therefore, the period of 1000 times positron bunch stacking is about 2.4ms. In a turn of the stacking ring, stacking is performed with three bunch intervals. In the next turn, stacking is not performed in the same bunch, but it is performed in the adjacent bunch which has 6.15-n-sec separation. This means stacking on the same bunch is performed with three turn intervals. The interval makes the stacking easier. Also through the process of the stacking, bunch spacing is changed from 18.5 ns to 6.15 ns. Since stacking takes long time, 2.4 m sec, cooling in the stacking ring is on going simultaneously. Remaining 0.9 m sec is used for additional cooling.

* The length of 132 bunches with 6.15 n sec spacing is 240 m, it is slightly shorter than the ring circumference of 260 m. Remaining 16 m is used for inter train gaps which is required for the cure of the electron cloud issue in the damping ring. The detail of inter train gaps in the stacking ring is not decided yet.

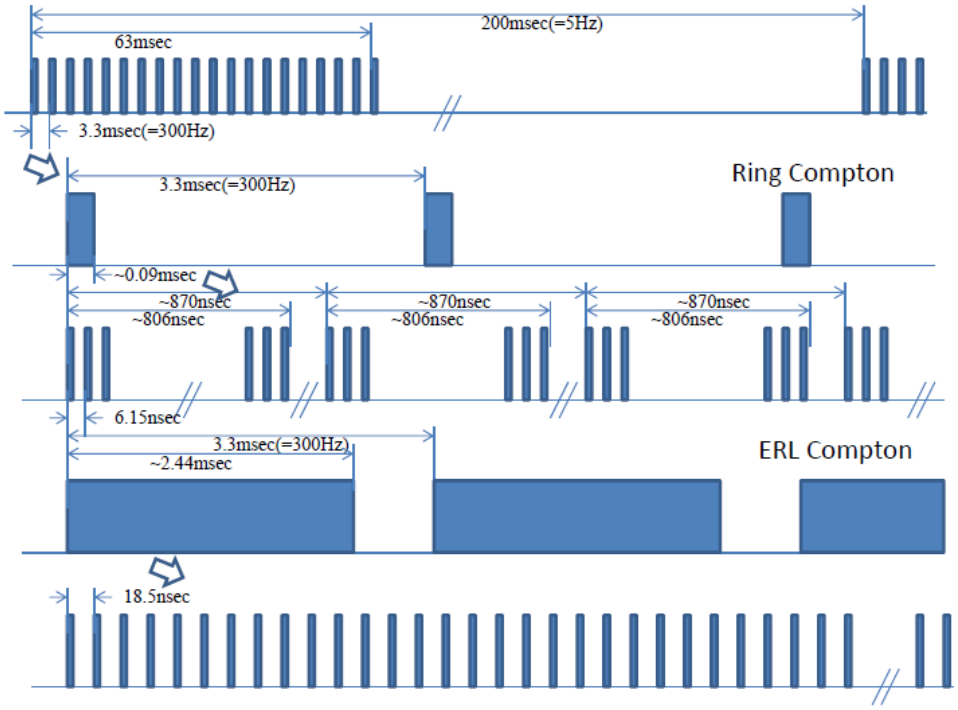

Fig. 3 The timing structure in the 5Hz superconducting linac for the stacking ring and in the 300Hz booster linac regarding Ring Compton and ERL Compton.

Reference:

Y. Ivanyushenkov et al, PAC 2007,Albuquerque, p2865.
A. Mikhailichenko, PAC 2007, Albuquerque, p1974.
E. Baynham et al, PAC 2009, Vancouver.
J. A. Clarke,
http://ilcagenda.linearcollider.org/getFile.py/access?contribId=462&sessionId=77&resId=0&materialId=slides&confId=4507, IWLC 2010, Geneva.
G. Ellwood,
http://indico.cern.ch/getFile.py/access?contribId=6&resId=0&materialId=slides&confId=109166, EUCARD-WP7-HFM collaborationmeeting, Nov 2010, CERN.
S.P. Antipov et al., PAC 2007 Albuquerque, p2909.
I.R. Bailey et al., EPAC 2008, Genoa, p715.
I.R. Bailey et al., IPAC 2010, Kyoto, p4125.
I.R. Bailey,
http://ilcagenda.linearcollider.org/getFile.py/access?contribId=485&sessionId=83&resId=0&materialId=slides&confId=4507, IWLC 2010, Geneva.
J. Gronberg et al, IPAC 2010, Kyoto, p4137.
J. Gronberg, KILC12
Wanming Liu and Wei Gai, IPAC 2010, Kyoto,p4134.
Wanming Liu and Wei Gai IPAC 2012
T. Omori et al., Nuclear Instruments and Methods in Physics Research A **672** , 52–56(2012).
M. Kuriki et al., ILC positron source based on laser Compton. AIP Conf. Proc., 980:92–101, 2008.